Large Solar Arrays -The Emerging Space Power Workhorse

J. E. Boretz
TRW Systems

LARGE SOLAR ARRAYS
THE EMERGING SPACE POWER WORKHORSE

by

J. E. Borets, Sr. Staff Engineer
TRW Systems Group
Redondo Beach, California

Abstract

The solar array/secondary battery system has emerged as the space power "workhorse". Previously considered only for applications of up to 1 KW_e arrays of up to 3 KW_e have been flown. Even larger arrays (10 KW_e) are being developed for Apollo Telescope Mount (ATM) and the "wet" Orbital Workshop. An Earth Orbiting Space Laboratory (EOSL), in the planning state for a 1973-1975 flight readiness date, is considering the use of a 38 KW_e solar array system. A 50 KW_e array is under development for an electric propulsion mission and a 45 KW_e array is in the conceptual design phase for a lunar surface application. Finally, a study has been initiated to assess the practicability and cost effectiveness of utilizing a 1 MW_e array for earth orbital applications.

An intense technology development program has been underway for several years. The emphasis has been on solving problems that relate directly toward utilization of large solar arrays. These have included light weight structures, improved power distribution and cost reduction techniques. This paper discusses the various approaches being taken by both government and industry to resolve these problems.

Introduction

One of the most important subsystems associated with spacecraft for both Earth orbital applications and planetary exploration is the electric power system. For long duration missions, solar cell technology has evolved to a level of performance so that solar arrays have become the workhorse of space power systems. This can be attributed to three major factors. First, it possesses the virtue of being a static system with inherent redundancy due to the multiplicity of cells, strings, and modules comprising its power conversion element. Secondly, by converting the sun's radiant energy into electricity by means of a zero cost, heat source whose constancy, life, and reliability are unequaled by man-made alternates. Finally, its only potential competitors, i.e., reactor or isotope heat source power systems, have suffered from a long history of technological and system effectiveness problems. These have included high temperature materials deficiencies, corrosion, heavy shielding, limited life, high cost, and safety and operational hazards due to the nuclear radiation by-product. As a result, mission planners operating within the constraints of technology readiness, are not prone to take the development risks associated with these nuclear systems.

Solar arrays first achieved eminence in 1956 when conversion efficiencies of 6 percent were realized thereby deflecting interest away from solar dynamic systems. Now, because of improved design and manufacturing processes, efficiencies of 10 to 12 percent are the norm. The overwhelming success of these single crystal silicon cell systems in power ranges up to the multi-kilowatt level, undoubtedly assures their continued use in future spacecraft applications.

In assessing the various factors affecting the use of large solar arrays for various long duration space applications one is initially confronted with an overwhelming set of parameters. This evaluation is further compounded by the various technical disciplines involved. Finally, the various performance, design, and operational criteria are so intimately interdependent, that a detailed systems engineering approach is required to arrive at the most system effective solution. Therefore, perhaps the major technological problem confronting both Government and industry today, is to develop an all encompassing, standardized, methodology for solar array design. The need for the generation of such an analytical model is long overdue.

Therefore, this paper, in addressing itself to the technological problems associated with long duration solar array operations in space, reflects only the limited perspectives existing today. As such, its main emphasis is upon identifying the challenges confronting the solar array designer rather than providing specific solutions. However, the current technical approaches being taken are outlined and their effectiveness in enhancing the technology readiness of solar array systems is discussed.

Design Constraints

The major factors affecting solar array performance and design are the environmental criteria (reference 1) and the operational modes. For long duration space operations, the impact of these conditions is to reduce solar array end-of-life (EOL) performance, impose severe material selection requirements, and introduce increased system complexity. If the solar array power level is high, i.e. up to 50 KW_e, additional problems associated with stowage, deployment, and spacecraft interactions also can occur. It is important, therefore to recognize the unique mission dependency of each solar array design. However, if one limits oneself to the basic elements comprising a solar array system, namely; the cellstack, substrate, and power distribution system, then many regions of technological commonality can be identified.

The discussion in this paper is constrained to a review of only those technology problems related to the performance and design of the cellstack, substrate, and related power distribution elements.

Solar Array Performance Considerations

There are various factors which affect solar array performance. These can generally be

classified into two groups. These are:

- time independent factors
- time dependent factors

The first group are independent of mission duration. They are primarily a function of the basic cellstack electrical characteristics, array design and manufacturing techniques, and operational criteria. They are initially determined by experimental evaluation and an analytical assessment of the impact of the spacecraft operating constraints. The latter requires a detailed thermal analysis to establish actual solar cell conversion efficiencies, an assessment of array orientation accuracy, and shadowing losses. The resulting array performance determined from applying these factors, is referred to as the beginning-of-life (BOL) power output.

The second group are intimately related to the space environment and the elapsed mission time. In order to assess the impact of these factors on solar cell performance degradation, a priori knowledge of this space environment is required.

All these factors must also be evaluated. Taken together with the time-independent factors, they establish the achieveable EOL power-to-area ratio. The relationship used to determine the power-to-area ratio from these factors can simply be expressed as:

$$\frac{P_o}{A} = \left\{\eta_p\, \eta_c\, \eta_m\, \eta_o\, \eta_{REG}\right\}\left\{\eta_{tc}\, \eta_{RAD}\, \eta_{uv}\, \eta_{mm}\right\}$$

$$\left[\eta_{CONV}\right] f_{(T)} \left[\frac{I_{SOL}}{I_{(AU)}}\right] \qquad (I)$$

These factors are defined in Figure 1. The solar intensity, I_{SOL} will vary inversely as the square of the distance from the sun. At 1 AU and AMO, its value is estimated at 139.6 mw/cm^2. Typical electrical performance characteristics for some commonly used N+ on P silicon solar cells at 28°C is shown in Figure 2. It should be noted that higher voltages and maximum optimum power are obtained with the lower base resistivity (2 ohm-cm.) cells. However, for both the 2 ohm-cm. and 10 ohm-cm. cells, as thickness of the cell is increased, the output of the cells increase. Thus, for a given base resistivity cell, the greater the thickness, the higher the cell conversion efficiency (η_{CONV}). This can be seen from the data plotted in Figure 3. However, since it is a high power-to-weight ratio that is desired, rather than high conversion efficiency per se, the thinner silicon cell is to be preferred. This is also shown in Figure 3, where for a constant cover glass thickness of 6 MILS, a 2 ohm-cm., 10 MIL silicon cell with an efficiency of 11.1% has a power-to-weight ratio of 200 W/Kg (~75 W/lb). A 6 MIL cell with similar characteristics and an efficiency of 10.1%, however, has a power-to-weight ratio of 275 W/kg (~100 W/lb). Furthermore, if CdS thin films are considered, even higher specific powers (up to 375 W/Kg) are projected for conversion efficiencies as low as 3.5%. In both instances, however, technology problems may preclude the use of these higher power-to-weight ratio cells.

For example, the cost of the 2 ohm-cm, 4 MIL silicon cells is considerably higher than that for 10 ohm-cm, 8 MIL cells. If a conservative price differential of $4/cell is assumed and recognizing that approximately 15000 to 20,000 cells/Kw are required depending upon the cell efficiency, a cost penalty of $60,000 to $80,000 per kilowatt results. Decreased handling durability and lower availability further mitigate against use of the thinner cells at this time.

The current status of cadmium sulfide (CdS) thin film cells is reported in Reference 2. Despite intense development efforts over the last few years, the CdS thin film cell is still plagued by many development problems. These include low performance due to inability to control reproducibility techniques, instabilities due to thermal cycling, and degradation in performance due to humidity effects, and thermal vacuum storage at 100°C. Until these foregoing technology problems have been resolved, the CdS thin film cells cannot be recommended for use at this time. However, the long range potential for reduced cost and high power density justify sustained development effort in this area.

The impact of temperature on cell electrical performance, is another major factor affecting the solar array power-to-area ratio. As the cell equilibrium temperature increases from a nominal 28°C to values approaching 60°C for earth orbiting applications, (Figure 4) and 95°C for lunar surface applications (Figure 5), a marked decrease in cell conversion efficiency (η_{CONV}), occurs (Figure 6). The net effect is that the array must be sized based upon the reduced power-to-area ratio resulting from the peak array equilibrium temperature. In some instances, time oriented load profile matching can be utilized to minimize the impact of this performance degradation factor on the array design. In addition, because of albedo effects, solar arrays for low altitude earth orbital missions and lunar surface applications result in higher equilibrium temperatures than for synchronous orbit and away from the sun (greater than 1AU) interplanetary flights.

For long duration operation the deliterious effects of the space radiation environment presents an even greater technology problem than that associated with temperature. Despite the fact that array performance degradation at BOL is significantly affected by array equilibrium temperature, the magnitude of this effect can be fairly accurately predicted. In addition, experimental confirmation of this effect can be fairly easily obtained in the laboratory. The space radiation environment, on the other hand, represents a region of high uncertainty. The radiation environment encountered in space consists of charged particle radiation and the solar illumination intensity. The charged particle radiation is composed of galatic cosmic rays, solar-protons and electrons. While the galactic radiation maintains a relatively constant level with time, the charged particle radiation rises occasionally by several orders of magnitude during solar flare disturbances. Normally, this solar flare activity is directly related to sunspot quantity. Figure 7 depicts the number of sunspots observed or predicted for three 11-year solar cycles. It should be noted that for missions occuring in the 1971 to 1976 time period a minimum of solar flare activity is anticipated. Missions conducted during the 1976 to 1981 time period may encounter maximum activity. To assess the impact of charged particle degradation on solar array performance the integrated flux must be determined on a statistical basis from space environmental data of the type

available in Reference 1.

The solar spectrum also varies and is considered to follow that of Johnson for AM0 and 1.0 AU (Reference 1). During periods of high solar activity, the x-ray flux may increase by 1 or 2 orders of magnitude. Generally, its value is in the 10^{-8} to 10^{-11} w/cm^2 range in the region from 100Å to 2Å respectively. This together with the ultra-violet portion of the solar spectrum will contribute to solar array performance degradation.

The meteoroid flux and the resultant impact on solar array performance is even more difficult to predict than charged particle radiation effects. The flux can vary widely and erratically as a function of time due to sporadic showers, and its particle sizes, distribution, and velocities can only be evaluated on a statistical basis at best. In addition, secondary ejecta caused by micrometeoroid impacts can result in additional array performance degradation. Also, the actual effect of a strike on a cell or a string of cells is subject to wide variations. Fortunately, experience to data with orbital, interplanetary, and lunar surface spacecraft has not substantiated the degradation values predicted by analytical estimates. However, as solar array areas increase for higher power requirements and mission durations are extended up to ten years, the probability of greater potential damage will be ever present.

Despite the uncertainties associated with the evaluation of the various degradation factors outlined above, the feasibility of using large solar arrays for long duration missions is not in question. Conservative assumptions and judiciously selected component trade-offs can assure a high probability of meeting solar array EOL requirements. Rather, the challenge lies in identifying problems and providing solutions to those technology areas which would result in major reductions in array weight and cost, and in increased reliability.

Solar Array Cellstack Considerations

The theory of the photovoltaic energy conversion process has received increasing attention during the last two decades. The highly successful application of solar arrays for spacecraft power systems has been one of the major factors in accelerating this interest. A fairly recent review of the various theories devised to analyze this process and a discussion of the experimental efforts engaged in to confirm these analyses is given in Reference 3. A short summary of the state-of-the-art of various solar cells is given in References 2, 4, and 5.

The solar array cellstack consists of various components and materials needed to generate the electric power required and to assure satisfactory operation in the hostile space environment. Typical silicon cell and CdS thin film solar cellstacks are shown in Figure 8 and 9 respectively. In selecting a particular cellstack for a given mission environment and life, the following key elements must be considered:

- Solar cell type, thickness, and base resistivity
- Cover glass material and thickness
- Cover glass to cell adhesive
- Cell interconnect design, material, and thickness
- Solar cell to substrate adhesive
- Main power cabling configuration and material

The critical selection criteria and tradeoff rationale for specifying the requirements for these cellstack elements is fairly well established. However, as array power levels are increased and mission durations are extended, optimization of these elements from a weight, cost, life and reliability standpoint becomes more complex. A detailed discussion of this optimization process is beyond the scope of this paper. However, as a few of the more significant technology problems confronting solar array designers are discussed, their relationship to the tradeoff process will be outlined.

Solar Cell Performance Related Criteria

For large area arrays, the cadmium sulfide (CdS) solar cell (Figure 9) has the potential for reducing array weight and cost. It also shows promise for increasing array stowage efficiency and reducing electrical degradation caused by charged particle radiation (Figure 10). However, the relatively low cell conversion efficiency (3 to 5%), present operational stability problems in the space environment, and other factors outlined in Reference 2, preclude the selection of these cells for near-term missions (up to 1975).

The 2 cm. x 2 cm., N-on-P, single crystal silicon cell is currently the preferred type. Production quantities are also available in larger sizes (3 x 3 and 2 x 6 cm.). Cost per unit area generally decreases with cell area. Limited operational experience, possible increased handling costs due to breakage, and thermal differential expansion difficulties due to increased length have limited the use of these larger cells. However, as solar array areas approach 5000 ft.^{2} and larger, the use of 2 x 6 cm. cell will become increasingly more desirable. Therefore, it behooves both Government and industry to resolve the current technological problems limiting their use at this time. This includes reduced production and handling costs, and improved adhesives, interconnects, and substrate materials to minimize temperature induced design problems and to increase array reliability.

Silicon cell base-resistivity can usually be optimized by selecting for a specific mission, the value that results in the higher EOL power. The standard 10 ohm-cm cell has a somewhat higher charged particle degradation resistance than do 2 ohm-cm cells. The latter, however, provide the higher output power initially. For long duration missions, depending upon the total integrated flux, the initial higher output of the 2 ohm-cm. cells may be outweighed by the higher radiation resistance of the 10 ohm-cm. cell. However, on missions where the total equivalent 1 Mev e/cm^2 fluence levels are estimated to be low (<10^{15} e/cm^2) the 2 ohm-cm. cell may still be preferred (Figure 11).

There are other parameters which must also be taken into account before a final solar cell selection is made with respect to charged particle radiation degradation. These include cell thickness and cover slide thickness. For example, at BOL and to fluence levels of 10^{14} e/cm^2 (1MEV equivalent), cell output power increases as cell thickness is increased (Figures 11, 12, and 13), up to about 0.016 inch. This is due to a characteristic

of the photovoltaic energy conversion process. In the thicker material, the electron-hole pairs generated in the bulk material away from the junction, have a greater diffusion length to allow the minority carrier to reach the junction. This results in a higher power output. As the level of the charged particle irradiation is increased, the effective diffusion length decreases. The net result is that electron-hole pairs generated far from the junction will generally recombine before the minority carrier reaches the junction. Consequently, thin cells which initially have a lower output than thicker ones, eventually have the same output as can be seen on Figure 14.

The impact of increased cover glass thickness is to reduce the effective radiation level on the cell. This is shown in Figure 15 for both solar flare proton and trapped electron irradiation. Data presented in Reference 6 on the ATS-1 at AMO seems to indicate that beyond a thickness of 0.006 inch, the benefits achieved in reduced solar cell radiation degradation may be offset by other performance degrading factors (Figures 16 and 17) such as reduced illumination. This has not been borne out by previous experiments (Reference 7 and 8) conducted at AMI as shown on Figure 18. Thus, at this time, it cannot be stated with certainty that EOL power output from each cell will increase with increasing cover glass thickness.

From the foregoing, it is evident that the selection of the optimum cell and cover glass thickness is not straight forward. They are highly mission dependent and quite sensitive to the dictates of the criteria used to arrive at the figure of merit for the overall solar array. Such factors as power density, cost, weight, volume, and reliability also enter heavily into the decision making process.

Solar Cell Material Considerations

In addition to establishing the criteria for the desired solar cell performance characteristics, it is equally important to select the proper materials for the elements comprising the cellstack. Not only must they be compatible with the imposed environments, but they must also demonstrate long life and high reliability. Some of the more significant considerations are as follows:

Cell Contacts

Recent investigations (Reference 9) have found that solderless cells having titanium-silver (Ti_1Ag) contacts shown severe degradation when subjected to a combination of high temperature and humidity. They have also indicated that completely solder covered cells exhibit insignificant degradation as a result of such exposure. Conventional solder covered cells are obtained by dipping the cells into solder. This results in unnecessarily heavy cells with a solder thickness of 39 μm (0.0015 inch). The so-called "dip and sling" method has been developed to overcome this problem. Increased cell wetting (up to 96%) and reduced solder thicknesses results. Another approach, developed by Helitek employs a tin coating (95% Sn/5% Ag) of approximately 2 μm thickness on the back surface and 8 μm on the front contact areas. The weight penalty in this case was only 4% of that for conventional solder dipped cells but the temperature/humidity degradation resistance was equivalent. These techniques and other newly developed proprietary processes have eliminated this problem without incurring the earlier weight penalties.

Cover Slides

Cover slides perform three functions on solar array cellstacks:

- Shield cell from excessive charged particle degradation
- Protect cell from micrometeorite damage
- Reduce cell maximum operating temperature

The basic material selection criteria for cover slides are:

- Must not darken substantially when subjected to the space radiation environment
- Should possess a high infared emittance
- Reasonable cost

There are two materials which will meet these requirements. They are Dow Corning Microsheet No. 0211 and Fused Silica No. 7940. The advantage of the former over the latter is its lower cost. The disadvantage is its greater transmittance loss under x-ray exposure. Therefore, fused silica, due to its long term stability in the space environment is recommended for long duration missions. There still is a potential technology problem associated with their use. Cover slides are normally coated with interference filters. The outboard side may contain an anti-reflective filter of MgF_2. Laboratory tests have shown that MgF_2 will deteriorate under low energy proton bombardments causing substantial transmittance losses. The mechanism causing the deterioration is presently not fully understood. However, data from spacecraft in orbits with relatively high low-energy proton fluences have not yet confirmed the laboratory results. Hence, this phenomenon should be investigated further to determine its possible impact on future long duration missions.

The reflective filter is normally located on the cell side of the cover slide. It provides protection for the cell-to-glass adhesive. Two basic types of ultraviolet reflective filters are available; blue and blue-red. Blue-red filters can reduce the array temperature by an estimated 5°C. However, due to a relatively lower transmission efficiency, an overall reduction in power output of approximately 3% results. Due to this factor and their higher cost, the blue filter is normally utilized. Their main function is to prevent severe ultraviolet degradation of the cell-to-glass adhesive. A filter cutoff wavelength of 0.410 micron results in a 3% greater power output than one with a 0.435 micron cutoff. Since the effect of the lower cutoff filter on adhesive degradation is considered negligible, a blue reflective filter with a cutoff wavelength of 0.410 micron is usually recommended. Continued research in this area is recommended, however, since considerable performance gains may be achieved by improvements with this component. Also, additional experimental data is desirable to assure satisfactory operation for longer durations (up to 10 years).

Glass-to-Cell Adhesives

Adhesives for bonding cover slides to solar cells are predominately organic, high polymeric materials. The basic polymer resins are modified by the control of the molecular weight, degree of

cross-linking, and the incorporation of additives to improve specific properties. Changes in the chemical balance of the adhesive can lead to significant modifications to its physical properties. In the case of optical adhesives these can result in adverse effects to the adhesive refractive index or spectral transmittance, thus lowering the solar cell performance.

Adhesives of principal interest are epoxies and silicones. They have demonstrated superior ability to withstand ionizing radiation for long periods without any significant change to structural properties or optical transmittance. The most commonly used are the silicones, with GE/RTV602 and Dow Corning Sylgard 182 or XRG-3489 preferred.

The photochemical decomposition of these adhesives result in degradation of their optical properties, such as adhesive darkening and increased solar absorptance. Because the recommended silicones are capable of distributing absorbed ultraviolet photon energy along its polymer chain, the degradation of optical properties are minimized. Laboratory tests have shown that Dow Corning's XRG-3489 (a highly purified version of Sylgard 182), has the least coloration due to ultraviolet and charged particle irradiation. Data from satellite experiments have confirmed these results for time-integrated fluxes corresponding to 3 to 5 years at synchronous orbits. Thus, DC/XRG-3489 is currently considered the best selection for long duration missions.

Cell-to-Cell Interconnect Design

Minimum cost consistent with reliable performance dictates the choice of solar cell material. Candidate materials include copper, silver, kovar, and molybdenum. The materials are listed in order of increasing cost (material plus fabrication). Typical properties of some of these materials are shown in Table 1. Thermal expansion matching between the interconnect material and the silicon cell is an important consideration. However, the major technological problem confronting solar array designers for long duration missions, is that created by thermal cycling. This environmental phenomenon causes solder fatigue at the joint between the interconnect and the silicon cell. The solder having a higher coefficient of expansion than silicon is subjected to repeated tensile stresses during low temperature excursions. The result is fatigue induced micro-cracks in the solder which ultimately propagate into the silicon cell. Ultimately, separation between the materials occurs. This can cause a reduction in array power when the failures per cell exceed the built in redundancy. Since for many long duration missions a large number of temperature cycles may occur, it is most important that intercell connections be capable of surviving this effect.

It is recognized that the initiation of cracks can be used as an indice of eventual failure. Thus, the number of cracks observed can serve as a useful failure rate indicator. Tests at TRW Systems have shown that there is a general relationship between lower temperature limit, number of cycles, and the relative amount of cracks in the joint (Figure 19). It can be seen that a relatively small increase in the lower temperature limit will permit a large increase in the number of cycles for a given level of cracks. Thus, improved thermal control of solar arrays to increase the lower temperature limit can greatly increase array operating life.

The number of failed joints also varied greatly with the interconnect material used (85% for copper, 7% for Kovar, and no failures for molybdenum after 100 cycles to -175°C). There was also a significant correlation between failure rate and temperature differential. Another observation during this test evaluation showed that it is very important to have oxide free surfaces which are to be joined by soldering to assure good joints. It was also established that proper interconnect plating is important. However, temperature shock rate was not found to be critical for the designs considered.

Specimens tested included those in a freely suspended state as well as those bounded to metallic substrates with silicone adhesives. The bonded specimens using 0.003 inch thick material resulted in the highest failure rate. The differential contraction between the modules and the substrate was the main factor, but material thickness was also critical. Figure 20 shows that the percentage of failures, after 300 thermal cycles, rapidly decreases with reduced interconnector material thickness. This was attributed to the probability that the stress level in the 40-60, lead/tin solder was considerable reduced during low temperature excursions by the greater flexibility of the thinner materials. It was estimated that a stress reduction of 5% can reduce the number of failures by a factor of 5. Variations in the solder composition could also have a major effect on fatigue life and further investigations in this area is recommended.

The tests confirmed that a U-shaped, Kovar interconnector, 0.001 inch thick can withstand 300 temperature cycles from 60°C to -162°C with only 0.7% of the joints separating. A 70% reduction of the stress in the solder joint can be achieved if the -162°C lower temperature limit could be raised to -115°C. For an equal number of temperature cycles (i.e. 300), the number of failures would then be reduced by several orders of magnitude. This can be seen in Figure 21 which shows the percent of cracks as a function of the average stress-to-failure, for a range of standard deviations of fatigue strengths for solder. The range of standard deviations shown brackets the range normally experienced in practice. If, on the other hand one assumes the percentage of open joints to be constant, several orders of magnitude increase in the number of allowable temperature cycles should result.

Solar Cell to Substrate Adhesive

The selection of the solar cell to substrate adhesive should be made when the actual substrate structure has been defined. There are a wide variety of suitable adhesives available. For bonding to aluminum face sheets, GE/RTV-511 or 577 is typical. To satisfactorily bond to Kapton, GE/SMBD 745 flexible epoxy adhesive is recommended. Adhesive thickness and bonding pattern should be established by pull tests conducted for the particular environmental levels associated with the particular mission.

Main Power Cabling

The selection of main power cabling design is intimately related to solar array power and voltage levels, as well as required stowage and deployment techniques. Material selection should

be based upon optimization with respect to the following parameters:

- Electrical Conductivity
- Weight
- Solderability
- Environment
- Thermal Conductivity
- Manufacturing Complexity
- Tensile Strength
- Cold Flow Characteristics and Flexibility

Table 2 summarizes several of these parameters for several candidate bus materials. A column indicating a relative weight multiplier for the various materials as compared to copper is included. While aluminum looks attractive, its high coefficient of thermal expansion is not too compatible with large thermal cycling excursions. Copper still remains the most satisfactory alternative.

Designating the main power conductor for constant current-density power transfer results in the lightest weight regardless of allowable power loss or operating voltage (Reference 10). Figure 22 is a schematic representation of a multi-winged spacecraft. Each wing consists of several identical electrical sections interconnected in parallel to deliver a specified array power and voltage. For a constant current density cable:

$$\text{Total Wing Power Loss} = K_1 N(N+1) \quad (2)$$

$$\text{Total Wing Conductor Mass} = K_w N^2 (N+1)^2 \quad (3)$$

Where,

$$K_1 = \frac{\rho L (\frac{P}{V})^2}{A_1} \quad (4)$$

$$K_2 = \frac{\rho D L^2 (\frac{P}{V})^2}{\text{Total wing power loss in watts}} \quad (5)$$

And,

P= Individual section power (constant)
V= Array Operating Voltage
ΔV= Voltage drop between each section and the spacecraft
N= Number of sections
L= Conductor Length between sections (constant)
A= Conductor cross-section, (in^2)
ρ= Material resistivity (Lohm-cm)

Conductor geometry (i.e., conventional wire or flat strap) selection is based upon the specific solar array structural design and deployment concept being used. The flat strap type is preferred for large area solar arrays since it is compatible with both rigid and flexible designs. It also has the potential for optimization with respect to weight, stowage efficiency, launch survivability, reliability, and cost.

Solar Cell Design Considerations

There are many solar cell design techniques that can markedly effect array performance, life, and reliability. A few significant technology areas are discussed below.

Magnetic Field

A major consideration during the period of design when the arrangement of series strings on the substrate is being established is that of minimizing the magnetic field caused by uncompensated current paths on the array. Both the arrangement of series strings and the location of the main power cabling must make maximum use of current counterflow loops. In this way, magnetic interference from the array circuit can be reduced to negligible levels (approximately 1 pico tesla).

Array Output Prediction

Solar array output calculations are normally made for the nominal output. This means that the median value of each degradation factor is used, thus resulting in a 50% probability that the predicted output will actually be achieved. This is done to avoid using an unnecessarily conservative EOL performance factor-of-safety with a correspondingly heavy design. Reference 11 describes a technique by which the power output at any desired probability may be determined. This technique utilizes the Monte Carlo method of selecting the magnitude of the degradation factors. The performance is then calculated at the particular operating voltage being considered. Figure 23 shows a typical set of curves (based upon a specific set of degradation factors and where $K=V_{OP}/V_{OC}$). Data of this type can be used to determine the array output at any desired probability, thus aiding materially in refining array sizing operations. TRW Systems has determined that the power output expected with 50% probability is approximately 7% higher than that anticipated at 95% probability. Thus, an increase in array size by about 7% above the nominal design, will assure a high probability that the EOL required power can be achieved.

Low Energy Proton Protection

As additional operating experience is obtained for long duration satellite systems, new technology problems occasionally arise. One such case is the excessive damage caused to uncovered portions of solar cells by low energy protons. Recent data from the ATS-1 Satellite, which has subsequently been verified by laboratory tests, have shown this to be the case. The damage mechanism is hypothesized as having a shorting effect on the solar cells. This has resulted in a power output degradation of 23% in one year. This was far in excess of the exposed cell area of 0.7% which being uncovered, would be the only region where rapid radiation damage would be anticipated. In the ATS-1 application, the cells used were 1 cm. x 2 cm., N-on-P type, with solder covered contacts. The negative contact was along the 2 cm. side. These cells were covered with 0.030 inch thick fused silica cover slides. Because of the standard tolerances on the cover slide and the assembly techniques used, a 0.005 inch wide strip along the 2 cm. length remained uncovered. Preflight degradation estimates for this condition were estimated at 2% per year. The unexpected damage was attributed to low energy (E<5 MEV) protons which damaged the exposed cell area. It was found that at fluence levels of 10^{13} p/cm^2, a shift in the characteristic current-voltage curve knee occurred, resulting in a 25% decrease in the maximum power output. This large drop in performance was experienced despite the fact that the exposed area of each cell was only 0.4% (0.003 in. x 0.788 in. = 0.589 in^2 x 100). It

was determined that satisfactory protection from this degradation mechanism can be achieved by the application of a thin layer of protective material over the exposed area.

There are several methods that can be used to eliminate the exposed cell area. One low cost technique is to apply a thin layer of the cover slide adhesive to the exposed areas when using cover slides with conventional dimensions and tolerances. This operation can be performed to the solar array panel after final assembly. This adhesive is acceptable since it will not decrease transmissibility at BOL. The extent of ultraviolet darking of the exposed adhesive at EOL has yet to be determined. However, even if transmissibility was reduced to zero (100% darkening) less than a 1% reduction in output power would be experienced. Further testing is recommended to assure that the low energy proton protective capability of this adhesive is not significantly diminished as a result of longer duration operation.

Another approach would be to use oversize cover slides to completely eliminate all exposed areas. This method, although very effective is considerably more costly than the first approach. This results from the tighter tolerances required and the higher reject rate to be expected because of this.

Lithium - Diffused Radiation Resistant Cells

As was previously discussed, charged particle damage (Reference 12) remains one of the major factors in solar array performance degradation. Recent research in solar cell technology has led to the development of the lithium diffused radiation resistant cell. These cells have been shown to have a definite ability to recover from radiation damage (Reference 13). There is, however, a considerable lack of understanding regarding the nature of the radiation-induced defects in lithium doped silicon and the annealing process. Figure 24 shows a comparison between changes in the diffusion length for a lithium-doped cell and a control cell under 1-MEV electronic bombardment. Both cells were made from the same silicon wafer. Irradiation was stopped periodically and the cells were allowed to anneal at room temperature for the time periods indicated. It is theorized that the damage site involves a pairing between a defect and a lithium ion. The recovery mechanism then involves the diffusion on another lithium ion to the damage site and its pairing with the lithium-defect complex. It has been established that the speed and extent of recovery are strongly dependent on the amount of free or unpaired lithium. There is some evidence that a cell structure which incorporates a diffused phosphorus layer next to the junction (i.e. between lithium - diffused region and P-region) to give a three-layered p/n/n structure, results in a cell with improved radiation resistance without sacrificing the ability to recover. While high efficiency (13 to 14%) lithium doped cells have been produced, on the average they appear to have lower efficiencies than comparable cells without lithium doping. Effects of elevated temperatures and long term exposure to hard vacuum require further investigation before these cells can be given serious consideration.

Shadowing Effects on Solar Cells

For various missions, frequently portions of the solar array are shaded by structural elements such as antennas, booms, or portions of the spacecraft. Such shadows are usually time varying and of complicated geometry. Accurate knowledge of the output losses is required for a precise determination of the actual array power output, as well as for assessment of bus voltage variations, ripple, and RF noise.

Because of the electrical characteristics of solar cells, the losses are not proportional to the projected shaded areas, but are greater. This is due to two factors. The shadowed cells which are in series with illuminated cells block the current flow in the entire series string. Shadowed cells in parallel with illuminated cells shunt part of the generated current. Current flow blocking may be minimized by installing so-called shunt-diodes across cell groups. Shunting can be reduced by dividing large parallel groups into small ones and connecting each group through a so-called blocking diode to the bus. This diode isolates shadowed groups of cells from illuminated ones and thereby prevents shunt current losses.

In estimating performance and designing the cellstack circuitry for the solar array, these shadowing effects must be taken into account. The use of mathematical models of the type outlined in Reference 14, can greatly simplify this complex analysis and still provide the desired accuracy for the array output power estimate.

Solar Array System Considerations

Because the power level requirements of future spacecraft are continually increasing, considerable emphasis is being placed on the structures and mechanisms technologies needed and voltage level selection, for large area, high power, light weight solar cell arrays. Typical of these are some of the development activities outlined below.

Solar Array Substrate Design Criteria

The trend in photovoltaic solar arrays has been towards developing light weight, lower cost substrate structures. Emphasis has been placed upon increasing the power-to-weight ratio (w/lb). The folding modular and roll-up systems are essentially two basic solar array configurations which appear most likely to achieve these objectives. The necessity to reduce the substrate specific weight can best be seen on Figure 25. At higher array power densities, the maximum allowable structure-mechanism weight is reduced. Thus, for a selected cell stack design, an upper limit exists for array structural weight, if a desired power density is to be achieved.

Currently several major development efforts are being carried out. The most notable is the folding panel configuration being developed by The Boeing Company. An array power density of 20-24 w/lb. for a nominal 50 KW_e, 5000 ft^2 area system has been specified. This array uses silicon cells (8.6%, AMO, 55°C, 1 ohm-cm, 8 mil thick, 3 mil cover slides) mounted on a rigid substrate. The substrate consists of an edge frame and center spar made from 0.015 in. beryllium double box beams and a 0.003 in. x 0.2 in. woven fibre glass substrate. A specific weight of 21.8 w/lb. has been achieved. The substrate specific weight is approximately 0.16 lb/ft^2 which does not include the deployment mechanism.

Other companies actively engaged in light weight solar array development include TRW Systems,

Hughes, Ryan, Fairchild-Hiller, General Electric, and Electro-Optical Systems. EOS using electroforming techniques is endeavoring to develop a 40 w/lb. rigid silicon cell array. To achieve this high specific weight they are using 4 mil thick cells and 1 mil thick cover glass. These appear to be high cost elements and somewhat beyond the practical regime for current SOA silicon cell array fabrication techniques. The other companies (with the exception of TRW Systems) are under contract to JPL to develop a nominal 10 KW 30 w/lb. silicon cell roll-up array. Results to date are listed in Table 3. Details of their construction and the deployment techniques utilized are given in Reference 16.

TRW Systems has been concentrating on developing CdS thin film multi-kilowatt arrays in conjunction with an in-house program tied to the development of an electrically propelled interplanetary spacecraft. A typical design for a two-wing, 2.5 KW flexible structure solar array has achieved a specific weight of 27 w/lb, which includes the deployment mechanism. In addition, under contract to NASA/MSFC they are developing fold-up modules for lunar surface applications which show promise of achieving specific weights up to 40 w/lb.

Rotary Joint Power Transfer Mechanism

Large area solar arrays will require rotary power transfer mechanisms to permit roll-out type deployment and/or deployed array articulation. There are several methods by which this may be accomplished. These are:

- rotary transformers
- spiral wound continuous cables
- slip ring assemblies

Because of their specialized design requirements, rotating transformers are not considered practical at this time. Continuous spiral wound cables have limited life and impose an unnecessary limitation on degree of array articulation. They also result in relatively high power losses and overall power system weights. Slip rings appear to be the most attractive rotary joint power transfer mechanism available today. They combine light weight, low power losses, high reliability, and unrestrained articulation capabilities with relatively low cost and proven performance in the space environment.

Slip rings can be either of two types, i.e., pancake or drum, depending upon the design constraints imposed on the pancake dimensions. This solar array component is reliable, based upon over 150×10^7 vacuum operating hours. This data is the summation of a total of 54 space flown and laboratory tested units. Typical failure rate data is 6 failures/ring in 10^9 hours.

Power transfer from the array to the slip ring is accomplished through terminal strips or connectors. The power loss through the ring assembly depends upon the particular design. Typical losses are in the order of 0.25% up to at least the 10 KW power level. There are no apparent design restrictions which will prohibit slip ring designs for 50 KW or higher. However, there are several technology areas which will require further evaluation, if required by the spacecraft requirements, due to the lack of operational data. These are:

- use of multiple rotating joints (one for array deployment and another for array articulation)
- transfer of power voltages higher than 100 VDC
- operation at temperatures below -10°C

A considerable amount of detailed design information is available from Ball Brothers Research Corp. They have determined that power transfer at voltages above 200 VDC causes creepage between circuits. Corrona and/or electrostatic discharge are additional problems associated with high operating voltages. Close consideration must be given to ring spacing, dielectric insulation properties of materials, material degradation effects and the impact of increased power losses and noise. Normally, proper selection of barrier materials and increased circuit spacing are adequate to minimize any deleterious effects. This results in a negligible weight increase. If slip ring assembly envelope dimensions are not too tightly constrained, problems with high operating voltages can usually be eliminated.

Effective lubrication for low temperature operation is required. "Dry", compact composites having self-lubricating properties and good electrical conductivity are typical. These are usually metal based and contain small percentages of polytetrafluorethylene and a dry lubricant such as niobium-diselenide. This lubricating film transfers back and forth to heal any faults in the film. "Wet" films supplied by reservoirs, such as Ball Brothers "Vac-Kote or Esso's Poly-Scientific Division Univis P-38 oil are other lubricants commonly employed for space applications.

Space proven slip ring designs have operated for over 50,000 revolutions at speeds up to 60 RPM with negligible wear (based on examination of qualification test models). However, the slip ring assembly remains one of the most difficult single components of the solar array to design for long life and much further development effort is warranted.

Voltage Selection

Solar array weight optimization is influenced by other factors than component mass-density. Selection of the array operating voltage and allowable loss in the main power cable are two such design criteria.

The weight of arrays with shunt diodes continually decreases with increased operating voltage. This is due to two factors. The inherent high reliability achieved by the use of shunt diodes does not impose any appreciable weight penalty. In addition, the required main power cabling weight continually decreases with increased voltage. Omission of shunt diodes causes the system to have a discrete voltage at which the total weight is a minimum. Figure 26 shows the relationship among operating voltage, power level, and the predicted power loss (required over design) for this case for a reliability of 0.995. It can be seen that with a prescribed reliability level, the required over design increases rapidly with increased voltage. If shunt diodes are incorporated across each parallel cell sub-group the required over design is considerably reduced. For example, at a reliability of 0.999999, the required over design is approximately 0.1% and independent of voltage level.

The optimum voltage range without shunt diodes is between 100 to 300 VDC. With shunt diodes the range can be increased to from 500 to 1000 VDC. The actual optimum voltage depends upon the power level and allowable mutli cable losses. Above 1000 VDC finite but negligible weight reduction results with shunt diodes.

Solar arrays with shunt diodes operating at optimum voltage, are generally on the order of 10% lighter at 0.999999 reliability, than their alternative with a reliability of 0.995 for a 3 year mission. Reducing the operating voltage of a shunt diode protected array to the range for the alternative results in approximate weight parity but at a somewhat higher reliability. It is clear then that array voltage need not exceed 300 VDC for weight optimization. However, at a given power level and mission life, consideration of other factors such as relisbility, cost effectiveness, and circuit compatibility become important. For example, a shunt diode protected array results in an increse in array cost. Shunt diode unit costs (~$2), amplified by additional tooling costs and increased assembly time reduces their desirability. The cost effectiveness of their use must be weighed with respect to the requirements of each specific mission. In addition, even though total array weight decreases with increased operating voltage levels for the shunted configuration, practical considerations sometime preclude their use. Quite often the voltage level selection may be limited by power transfer mechanism, power conditioning, or load constraints.

For many applications there does not appear to be any significant advantage in operating solar arrays at voltages above 300 VDC. However, should the spacecraft load dictate the requirement (i.e. 2000 to 16000 VDC for electric thrustors and T.V. broadcast high frequency electron tubes) then techniques must be developed to make this achieveable. In this case, additional problems associated with interactions with the charged space plasma and increased spacecraft torques due to the impact of the magnetic field between the array and the plasma caused by incompensated current paths, must also be resolved.

Conclusions

The proven performance and reliability of solar arrays will make them the ideal electric power system candidate for the many potential missions being considered for the next decade. Because of their potential for high power, long duration operation, with minimum development risk, mission planners and spacecraft designers will turn increasingly towards their use.

The technology problems stemming from the desire to develop large, high power level solar arrays are primarily related to achieving improvements in the time-independent factors of BOL performance. The emphasis here is on increased solar cell conversion and power conditioning efficiency, improved manufacturing techniques and materials, and a refined assessment of spacecraft operating modes and solar array interactions. Development of light weight structures, and reliable deployment, orientation, and power transmission systems, (Reference 15) are equally important.

The technology problems related to the quest for extended mission duration are dominated to a large degree by the necessity of obtaining major improvements in the time dependent degradation factors. The development of increased radiation resistant materials is the key element to success in this area. Improved thermal control and decreased sensitivity to the range and magnitude of thermal cycling are additional factors that could enhance the reliability of long duration operation.

Finally, because of the multi-faceted aspects of solar array systems, increased emphasis must be placed on developing new analytical and experimental tools. These must be oriented towards achievement of major improvements in solar array design optimization techniques. Only in this manner can the basic objectives of reduced weight and cost, and increased reliability be achieved, to meet the future goals of long duration operation of large solar arrays in the hostile space environment.

References

1. R. E. Smith et al, "Space Environment Criteria Guidelines for use in Space Vehicle Development, 1967 Revisions"; NASA TMX 53521 dated February 1, 1967.

2. F. A. Shirland, A. F. Forestieri, A. E. Spakowski, "Status of The Cadmium Sulfide Thin-Film Solar Cell". IEEE/IECEC Conference, Boulder, Colorado; August 13-17, 1968.

3. P. A. Crossley, G. T. Noel, M. Wolf, "Review and Evaluation of the Past Solar Cell Development Efforts", RCA/Astro-Electronics Div. Report of December 1967 (NASA Contract NASW-1427).

4. P. Rappaport, "Solar Cells Today", AIAA/IECEC Conference, Los Angeles, California; September 26-28, 1966.

5. E. L. Ralph, "Solar Cell Development Survey"; IEEE/IECEC Conference, Boulder, Colorado; August 13-17, 1968.

6. R. C. Waddel, "Radiation Damage Shielding of Solar Cells on a Synchronous Spacecraft", IEEC Transactions/IECEC Conference; Boulder, Colorado, August 13-17, 1968.

7. K. S. Tarneja, R. K. Rial, J. M. Hicks, R. V. Babcock, "Drift Field Solar Cells on Silicon Web," AIAA/IECEC Conference, Los Angeles, California, September 26-28, 1966.

8. G. A. Haynes, W. E. Miller, "Effects of 1.2 and 0.30 MEV Electrons on the Optical Transmission Properties of Several Transparent Materials", NASA Technical Note TN D-2620; March 1965.

9. W. Luft, C. C. McCraven, and L. A. Aroian, "Temperature and Humidity Effects on Silicon Solar Cells"; Seventh IEEE Photovoltaic Specialists Conference, Pasadena, California, November 19-21, 1968.

10. TRW Systems Report 07171-6001-R000, "Power Systems Configuration Study and Reliability Analysis", JPL Contract No. 951574; of 18 September 1967.

11. W. Luft, "Solar Array Output Probability Predictions", TRW Report ER7442.6-073 of 24 May 1968.

12. R. L. Statler, "One MEV Electron Damage in Silicon Solar Cells," IEEE/TECEC Conference, Boulder, Colorado; August 13-17, 1968.

13. J. Wysocki, Record of 6th Photovoltaic Specialists Conference - Confidential, Cocoa Beach, Florida, March 28-30, 1967.

14. H. S. Rauschenbach, "Electrical Output of Shadowed Solar Arrays", IEEE Seventh Photovoltaic Specialist Conference, Pasadena, California; November 19-21, 1968.

15. D. W. Ritchie and J. D. Sandstrom, "Multi-kilowatt Solar Arrays", JPL Technical Report 32-1140 of 15 July 1967.

16. J. E. Boretz, et al; "Study to Establish Criteria for a Solar Cell Array for use as a Primary Power Source for a Lunar-Based Water Electrolysis System", Phase I - Final Technical Report of June 30, 1968 (TRW No. 09681-6002-R000-NASA Contract No. NAS8-21189).

Acknowledgements

This paper has been based in part upon the results of various studies and work (Reference 16) carried out by the author in the field of large area solar arrays. Supplementary data was provided by various members of the TRW Systems Electrical Systems and Physical Research Laboratories. This has included G. A. Work, W. Luft, R. A. Boring, H. S. Rauschenbach, J. M. Denny, and R. G. Downing. In addition, private conversations with A. Smith (NASA/OART) and R. Boehme and J. L. Miller (NASA/MSFC) aided materially in formulating the direction and emphasis to be taken in the preparation of this paper.

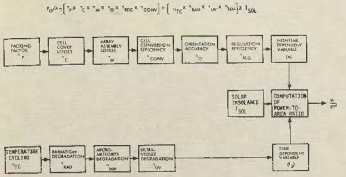

Figure 1. Factors Considered in Power-to-Area Ratio Computation for Lunar-Based Solar Arrays

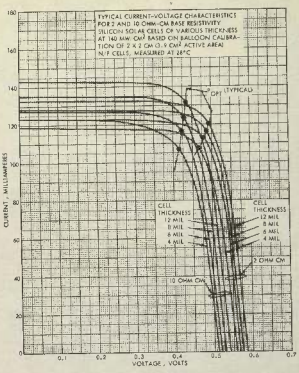

Figure 2. Typical Current-Voltage Characteristics for 2 and 10 ohm-cm Base Resistivity Silicon Solar Cells of Various Thicknesses

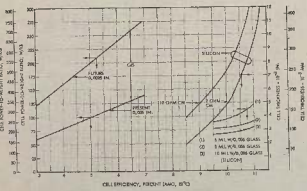

Figure 3. Power-to-Weight Ratio Versus Efficiency for Silicon and Thin Film Solar Cells

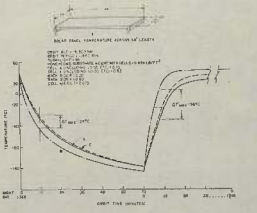

Figure 4. Temperature-Time Profile for Representative Panel

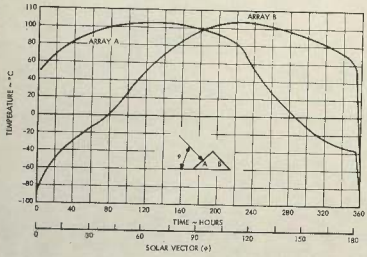

Figure 5. Lunar Based 45° Lean-To-Array Temperatures as a Function of Solar Heating Model I Unmodified

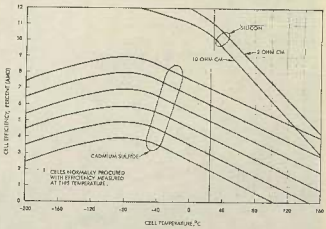

Figure 6. Cell Efficiency Versus Temperature Comparison for Silicon and Thin-Film Solar Cells

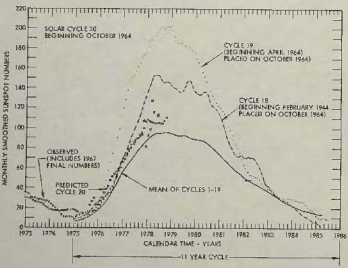

Figure 7. Sun Spot Numbers for Several Solar Cycles

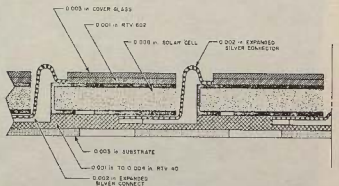

Figure 8. Advanced Solar Cell Stack Concept

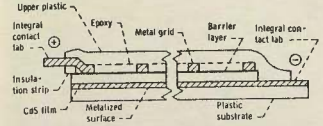

Figure 9. Cross-Section of CdS Thin Film Solar Cell

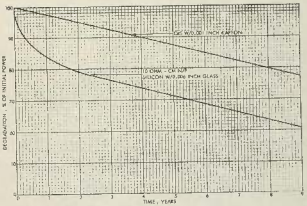

Figure 10. Silicon and CdS Thin Film Solar Cell Degradation due to the Space Environment

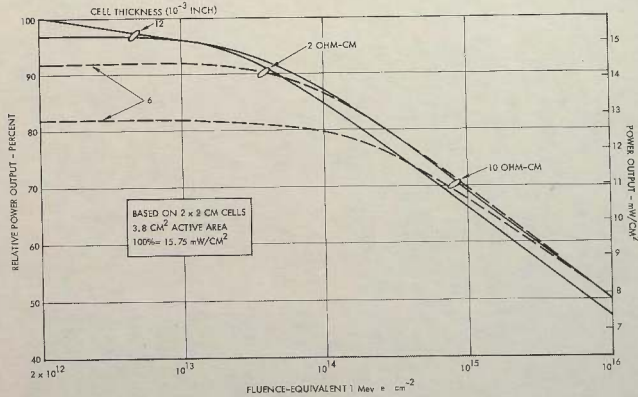

Figure 11. Effect of Fluence on Solar Cell Maximum Power for Various Cell Thicknesses and Base Resistivities.

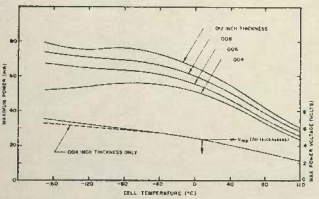

Figure 12. Maximum Power and Voltage vs Cell Temperature for 2 x 2 cm 10 ohm cm N+ on P Solar Cells, Active area 3.9 cm^2, Sunlight Simulator 140 mW/cm^2

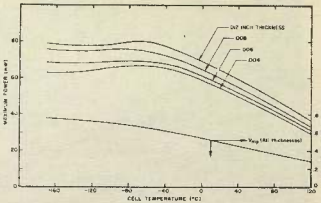

Figure 13. Maximum Power and Voltage vs Cell Temperature for 2 x 2 cm 2 ohm cm N+ on P Solar Cells. Active Area 3.9 cm^2, Sunlight Simulator 140/mW/cm^2

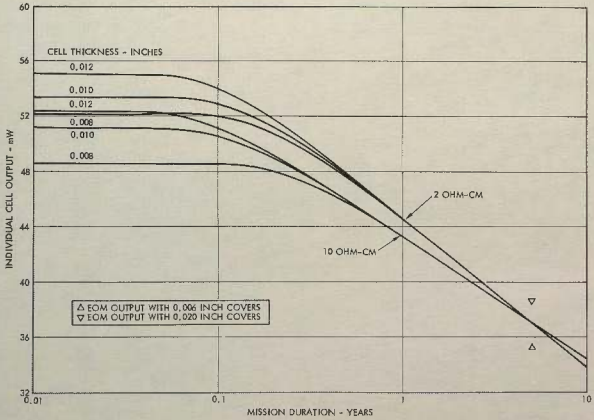

Figure 14. Individual Solar Cell Performance Versus Mission Duration for Various Thicknesses of 2 and 10 ohm-cm Solar Cells at AMO, 28°C for Bodymounted Cells which are Normal to Solar Irradiation and having 12 Mil Cover Slides. No Spacecraft Geometry Considered.

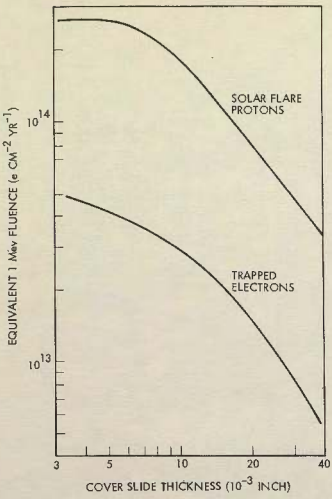

Figure 15. The Effect of Cover Thickness on the Yearly Solar Flare Proton and Trapped Electron Fluence in Terms of Equivalent 1 Mev Electrons, During Peak Solar Flare Period

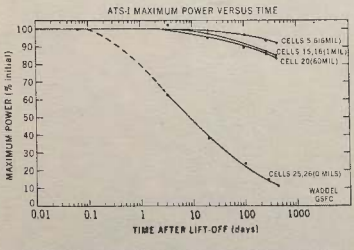

Figure 16. Maximum Power Versus Time for Several Cells with Various Shields

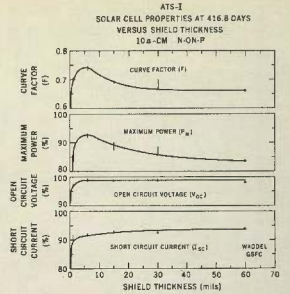

Figure 17. Curve Factor (F), Maximum Power (P_M), Open-Circuit Voltage (V_{OC}), and Short-Circuit Current (I_{SC}) Versus Shield Thickness, at 416 Days After Lift-Off.

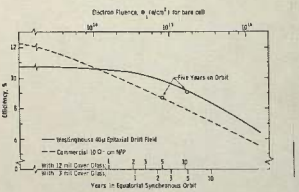

Figure 18. Solar Cell Efficiency Vs. 1 MeV Electron Fluence or Years Exposure in Equatorial Synchronous Orbit. Efficiency Measured with 3400°K Filtered Tungsten Light at 100 m W/cm^2, as Indicated on Standard Solar Cell Calibrated Table Mountain Sunlight

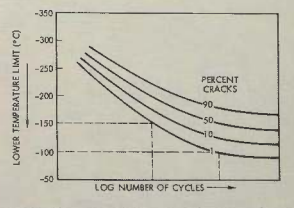

Figure 19. Typical Fatigue Life Curves for Solar Cell Interconnections

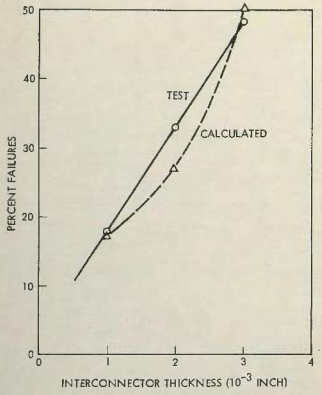

Figure 20. Solar Cell Joint Failure Level After 300 Thermal Cycles Versus Interconnector Thickness as Determined by Tests and by Calculations

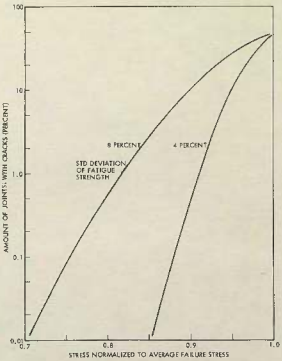

Figure 21. Cell Interconnect Joint Fatigue Cracks Versus Normalized Stress for Typical Range of Solder Fatigue Strength Distribution

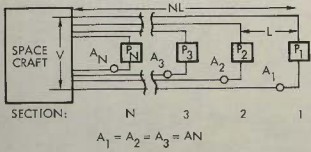

Figure 22. Schematic Representation of Solar Array Wing

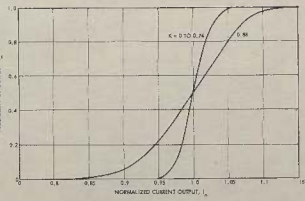

Figure 23. Dimensionless Current Output Distribution Over a Range of Normalized Voltages.

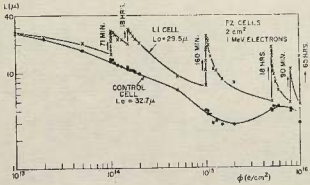

Figure 24. Comparison of the Performance of n/p and Li-doped Silicon Cells under Irradiation

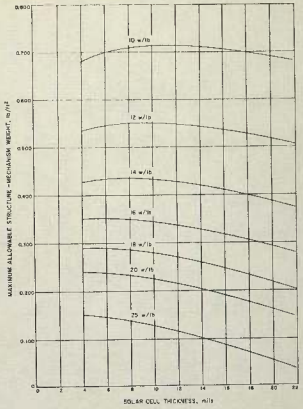

Figure 25. Allowable structures Weight (lb/ft^2) at Various Levels of Specific Power as a Function of Cell Thickness (For Mariner IV Cell Stack Specific Weight of 0.391 lb/ft^2)

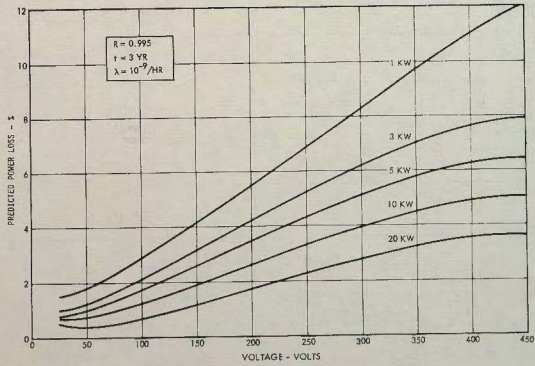

Figure 26. Effect of Array Operating Voltage on Power Loww for Silicon Cells at Various Power Levels (No Shunt Diodes)

Material	Relative Thermal Expansion	Density	
		lb/ft^3	m/cc
Silicon	1	151	2.33
Copper	4.1	555	8.89
Kovar	1.18	521	8.35
Molybdenum	1.20	562.5	10.20
Iridium	1.4	1400	22.42
Platinum-Iridium	1.87	1335	21.4
Tantalum	1.62	1036	16.6
Aluminum	4.6	168	2.7
Brass	4.9	527	8.44
Beryllium	3.5	113.5	1.82

Table 1. Comparison of Various Candidate Solar Array Electrical Interconnection Material Densities and Expansion Relative to Silicon

Company	Cell Type	Cell Thickness, in.	Cover Glass Thickness, in.	Cell Performance Characteristics	Array Specific Weight W/Lb
EOS	N/P	0.004	0.006	10.1%, AMO, 55°C	17
C.E.	N/P	0.008	0.003	8.45%, AMO, 55°C	10
Ryan	N/P	0.008	0.003	8.58%, AMO, 55°C	10
Fairchild-Hiller	N/P	0.008	0.003	9.3%, AMO, 55°C	14

Table 3. Comparison of Solar Array Specific Weights From Industry

Candidate Conductor Material	Resistivity (μ ohm-cm at 20°C)	Density (gm/cm^3)	Tensile Strength (Psi at 20°C)	Thermal Expansion Coefficient ($\alpha_C^{-1} \times 10^{-6}$)	Thermal Conductivity (W/cm°C)	Cold Flow	Solderability	Normalized Weight for Equivalent Power Loss	Magnetic
Copper (Pure)	1.69	8.94	28,000	16.6	3.89	Good	Very Good	1.0	No
Copper Alloy (Copper-Cisl Wire)	1.91	8.94	60,000	17.0	3.89	Good	Good	1.13	No
Silver	1.59	10.49	18,000	19.7	3.89	Poor	Very Good	1.1	No
Beryllium	4.20	1.85	50,000	12.0	1.47	Very Good	Poor	0.51	No
Aluminum	2.66	2.70	11-15.5K	23.8	2.09	Poor	Fair	0.48	No

Table 2. Summary of Candidate Bus Material Physical Characteristics